

pubs.acs.org/JPCA Article

Detecting Laser-Volatilized Salts with a Miniature 100-GHz Spectrometer

Published as part of The Journal of Physical Chemistry virtual special issue "International Symposium on Molecular Spectroscopy".

Alexander W. Raymond, Kin Long Kelvin Lee, Michael C. McCarthy, Brian J. Drouin,* and Eric Mazur



Cite This: https://dx.doi.org/10.1021/acs.jpca.9b10548

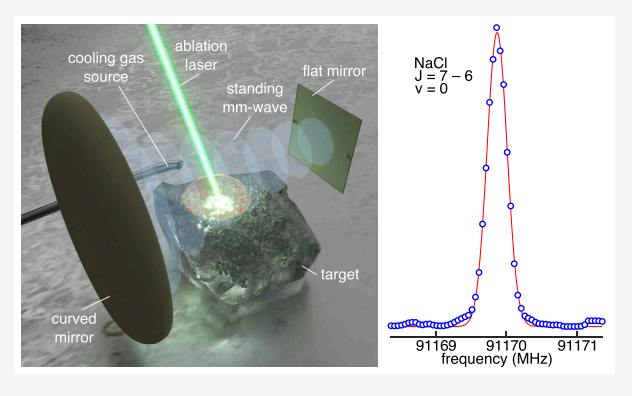


ACCESS

Metrics & More

Article Recommendations

ABSTRACT: Rotational transitions are unique identifiers of molecular species, including isotopologues. This article describes the rotational detections of two laser-volatilized salts, NaCl and KCl, made with a miniature Fourier transform millimeter-wave (FTmmW) cavity spectrometer that could one day be used to measure solid composition in the field or in space. The two salts are relevant targets for icy moons in the outer solar system, and in principle, other molecular solids could be analyzed with the FTmmW instrument. By coupling the spectrometer to a collisionally cooling laser ablation source, (a) we demonstrate that the FTmmW instrument is sensitive enough to detect ablation products, and (b) we use the small size of the FTmmW cavity to measure ablation product signal along the carrier gas beam. We find that for 532 nm nanosecond pulses, ablated



molecules are widely dispersed in the carrier-gas jet. In addition to the miniature spectrometer results, we present several complementary measurements intended to characterize the laser ablation process. For pulse energies between 10 and 30 mJ, the ablation product yield increases linearly, reaching approximately 10^{12} salt molecules per 30 mJ pulse. Using mass spectrometry, we observe Li^+ , Na^+ , and K^+ in the plumes of ablated NaCl, KCl, and LiCl, which implies dissociation of the volatilized material. We do not observe salt ions (e.g., $NaCl^+$). However, with 800 nm femtosecond laser pulses, the triatomic ion clusters Li_2Cl^+ , Na_2Cl^+ , and K_2Cl^+ are produced. Finally, we observe incomplete volatilization with the nanosecond pulses: some of the ejecta are liquid droplets. The insights about ablation plume physics gleaned from these experiments should guide future implementations of the laser-volatilization technique.

INTRODUCTION

Exploration of remote environments such as the icy moons of the outer solar system requires compact diagnostic tools that are preferably specific and quantitative. Spectral signatures at all wavelengths are exploited for such diagnostics; however, few techniques accomplish the specificity generally achieved by the measurement of gas-phase rotational transitions. Mass spectrometry, when coupled with liquid or solid vaporization techniques, has been the basic paradigm for specific characterizations of remote in situ systems, but basic uncertainties about sample volatilization and ionization dominate uncertainties in the data analyses. Ideally, the detection of neutral or transient species in the gas phase could also be done in situ and provide complementary knowledge of the samples under test. Building on recent progress in the miniaturization of millimeterwavelength (mm-wave) spectrometers that detect rotational transitions of gas-phase species, this work shows, for the first time, mm-wave spectra of laser-ablated solid measured using a miniature mm-wave device. The detection demonstrates the

complementary nature of rotational spectroscopy and mass spectrometrmetry for *in situ* chemical analysis.

This article reports two findings. First, it describes laboratory measurements of NaCl and KCl made by coupling a newly developed mm-wave Fourier transform spectrometer to a collisional-cooling laser-ablation source. Those measurements advance the feasibility of doing laser-ablation mm-wave spectroscopy to detect salts *in situ* on the icy moons of the outer solar system where subsurface oceans in contact with rock are thought to exist.² Second, the article reports a series of measurements that characterize the ablation plume produced when short laser pulses are focused onto a solid salt target. That characterization establishes the baseline for improving the

Received: November 10, 2019 Revised: January 28, 2020



laser ablation source in the future. In principle, the instrument we describe could be used to analyze other molecular solids including organics on icy moons and other solar system sites.

The instrument we use for the NaCl and KCl detections is novel—it incorporates a recently developed miniature Fouriertransform millimeter-wave (FTmmW) cavity detector called SpecChip.³⁻⁵ Millimeter-wave frequencies correspond to transitions between rotational energy levels and can be used to unequivocally determine the composition of the analyte, including isomers and isotopomers, based on the unique arrangement of atoms in the vaporized molecules.⁶ Pulsed carrier gas laser ablation sources like ours have been utilized by other laboratories to volatilize parent molecules for spectroscopic characterization^{7,8} or to facilitate molecular synthesis by ablating a metal target and seeding the carrier with a reactant. Such experiments are key for guiding radio-astronomical searches for new molecules, 12,13 and our measurements demonstrate that the same laser-ablation and carrier-gas collisional cooling techniques are viable means of volatilizing solids for in situ millimeter-wave spectroscopy. To date, only pyrolysis sources have been used to do *in situ* molecular measurements of solids in space. ^{14–16} A pulsed laser ablation source would have the advantage of high spatial resolution, which is beneficial for probing microscopic grains in planetary exploration. ¹⁷ A key aspect of the technology, which we demonstrate in this paper, is coupling a synchronized carrier gas isentropic expansion to the FTmmW cavity. The carrier gas collisionally cools the ablation products to reduce the rotational partition function and increase the line strengths.

The signal is proportional to the number of molecules in the FTmmW cavity, so future improvements to the instrument should focus on maximizing the volatilization yield from the ablation source. To that end, we perform a series of experiments to determine the properties of the ablation plume. By leveraging the fast transit of molecules across the small FTmmW cavity, we show the ablation products are spatially dispersed inside the carrier gas pulse. We quantify the volatilization yield for our nanosecond laser pulses using a laboratory microwave cavity spectrometer. Mass spectrometry without an auxiliary ionization source is done to identify positive ions. We observe atomic ions and, with 800 nm femtosecond pulse ablation, triatomic ion clusters. Scanning electron microscopy (SEM) imaging of salt particles collected on a coverslip shows that some of the material ejected from the sample remains in liquid state, indicating that the target is not fully volatilized. These characterizations of the ablation plume properties and the FTmmW detection of laser ablation products are important steps toward maturing the instrument for deployment in space.

METHODS

Figure 1a shows the experimental setup for the laser-ablation FTmmW instrument. A photograph showing the small size of the spectrometer can be found in our prior work. Laser pulses with 532 nm wavelength, 20 ns full-width-half-maximum duration, and 5-Hz repetition rate are used to volatilize the solid targets at pulse energies between 12 and 32 mJ. The calculated beam waist at the target is 150 to 250 μ m. The ablation source consists of a rotating/translating salt pellet, laser focusing optics, and a carrier gas valve with a 500- μ s long nominal pulse. Argon carrier gas is supplied to the valve at 650 to 1500-Torr absolute pressure and is synchronized to the laser. The FTmmW cavity and electronics have been described

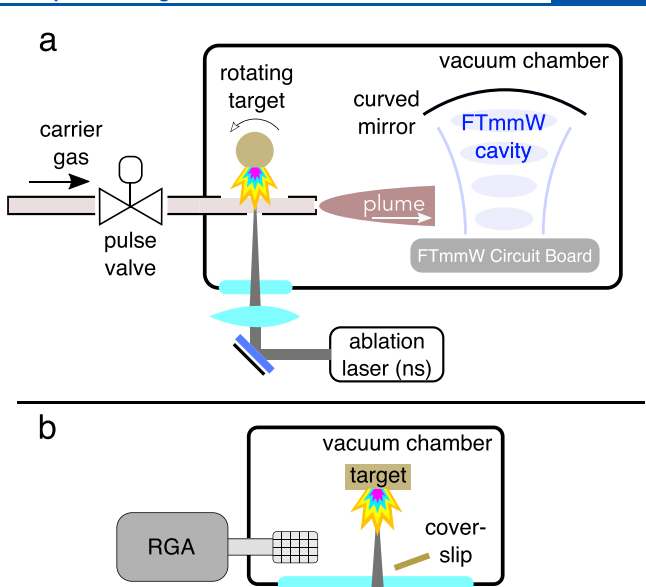


Figure 1. (a) Miniature FTmmW cavity spectrometer and the collisional-cooling laser-ablation source mounted in a vacuum chamber. The target is rotated and translated by a mechanical actuator to evenly ablate the surface. Pulsed carrier gas is used to collisional-cool the ablation products. (b) Mass spectrometry. This is done using a residual gas analyzer (RGA) operated in vacuum (μ Torr levels) without a filament ionizer, so ions produced by ablation are directly detected. Ablation with both nanosecond and femtosecond pulses is tested. The same setup is used to prepare samples for microscopy; a coverslip near the ablation target collects ejected particles.

moving

mirror

ablation

laser (fs)

ablation laser (ns)

previously.3-5,18 Briefly, the spectrometer comprises an amplifier/multiplier chain that generates mm-wave frequency radiation, a high-speed pulse former that sets the excitation pulse duration, a transceiver coupled to a semiconfocal cavity with a 50 mm diameter mirror where molecules are excited and radiatively probed, and a low-noise amplifier. The RF synthesizer that feeds the multiplier/amplifier chain is locked to a 10 MHz rubidium clock. The time-domain signal from the FTmmW chip is Fourier transformed using an oscilloscope. The lock-loop band is between 91 and about 102 GHz. The center of the FTmmW cavity is positioned approximately 100 mm downstream from the laser ablation source. A delay generator is used to control timing. The laser and mm-wave pulses are synchronized relative to the pulse valve. The laser is delayed about 430 μ s, and the 60 ns long mm-wave excitation pulse in the FTmmW cavity is delayed nominally 560 μ s.

The laboratory-scale Fourier transform microwave (FTMW) spectrometer used to quantify the ablation yields has been described previously. The ablation source in that setup is nearly the same as the one used with the FTmmW device except that the carrier gas is neon instead of argon and its flow rate is regulated by a flow controller to approximately 15 sccm. We find that the argon and neon carrier gases yield comparable signals. Emission line measurements of 100 to 500 repeated ablation cycles are averaged together. We calibrate yields using

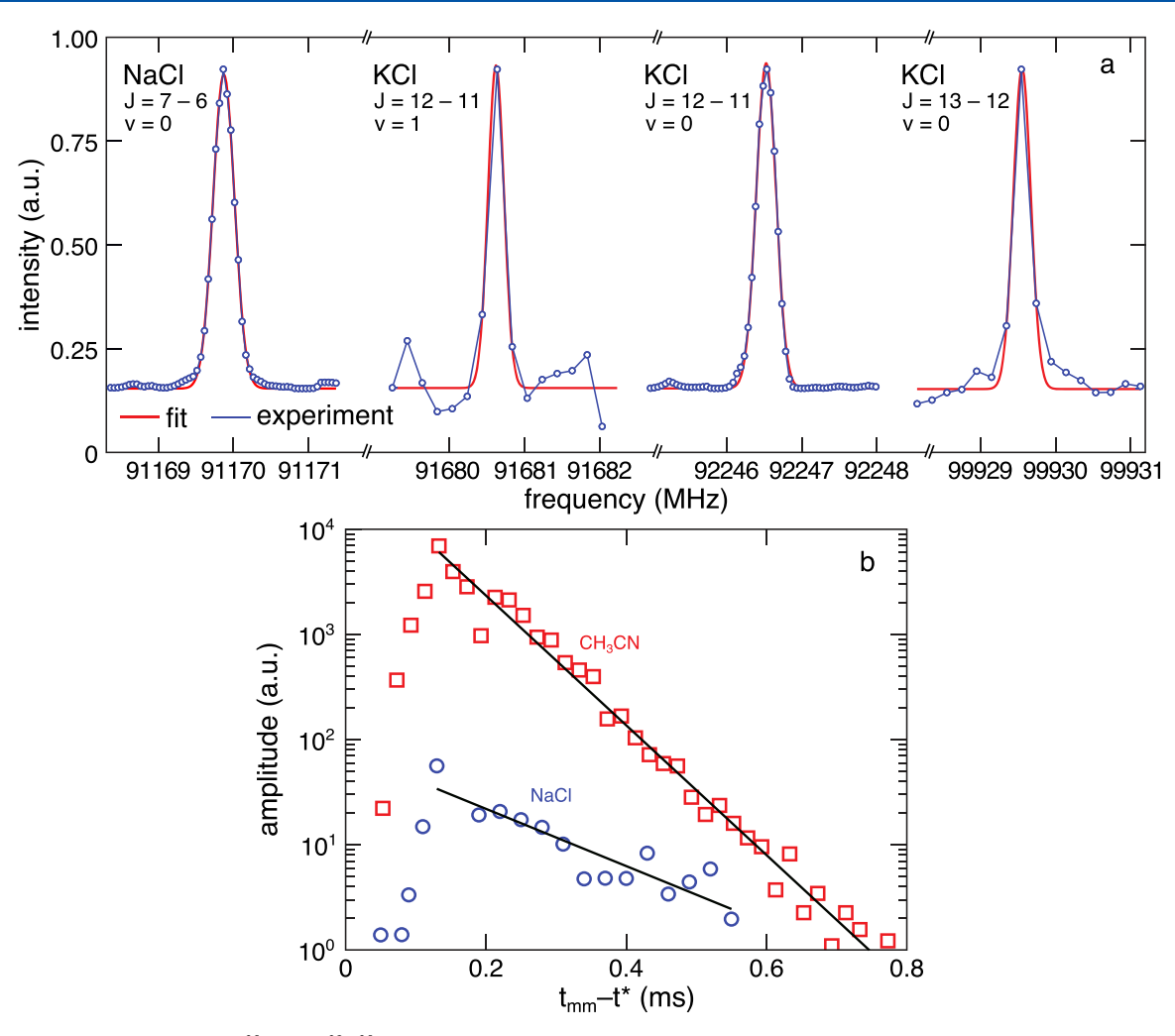


Figure 2. (a) Emission lines for Na³⁵Cl and ³⁹K³⁵Cl at the indicated vibrational states measured using the miniature FTmmW cavity spectrometer. (b) Na³⁵Cl emission line dependence on delay of the millimeter-wave excitation (at t_{mm}) compared to the laser firing (at t^*) with fixed carrier gas pulse timing. The J = 5-4 transition of the vibrational ground state of CH₃CN tracer gas (0.75% in Ne) at 91987.09 MHz is shown for comparison where t^* is the time when the laser pulse is set to release. Fits of the signal decays, $e^{-t/\tau}$, yield time constants of 120 μ s for NaCl and 40 μ s for CH₃CN.

the 12,256.584 MHz transition of SO₂ ($J_{K_aK_c} = 2_{02} - 1_{11}$) seeded at 0.5% in the carrier gas and using the relative strengths of rotation lines to determine the rotational temperature.

The mass spectrometry setup used to detect ions in the ablation plume is shown in Figure 1b. The mass spectrometer is a residual gas analyzer type with the entrance to the quadrupole mass filter positioned within 100 mm of the target. Positive ion spectra for both the nanosecond laser used in the rotational spectroscopy experiments and also an 800 nm, 100 fs laser were recorded at 1-kHz repetition rate. To avoid saturating the Faraday cup detector with ions, the laser fluence for the mass spectrometry test is intentionally limited to about 2 and 1 J cm⁻² for nanosecond and femtosecond pulses, respectively. The same setup is used to collect particles ejected from nanosecond pulses for SEM imaging. A glass coverslip overlaid with electrically conductive copper tape is positioned about 50 mm from the ablation target. Material ejected from the target lands on the copper, which provides an electrical path to ground to mitigate charging while SEM imaging.

The targets for rotational spectroscopy and particle SEM are prepared by compressing powdered salt (99% purity) with a

small amount of wax binder. For the mass spectrometry tests, vacuum epoxy is used instead of wax to bind the salt. Rotational transitions are inherently narrow, and we do not observe any signal from the binder near the frequencies of the salt transitions. Control mass spectra taken with only epoxy show only minor peaks.

RESULTS

Rotational transitions of laser-ablated NaCl and KCl detected using the FTmmW instrument are plotted in Figure 2a. The rotational constants for the salts have been characterized previously. 20,21 The center frequencies (and widths based on Gaussian fits) of the Na 35 Cl (J=7-6, v=0) emission line and the 39 K 35 Cl (J=12-11, v=1), 39 K 35 Cl (J=12-11, v=0), and 39 K 35 Cl (J=13-12, v=0) emission lines are 91,169.9 (0.3), 91,680.6 (0.3), 92,246.5 (0.2), and 99,929.5 (0.3) MHz, respectively. These center frequencies agree with catalog values to the reported precision. 22 In Figure 2b, the amplitude of the Na 35 Cl and CH 3 CN tracer signals are plotted versus the mmwave pulse delay relative to time the laser pulse is set to release. At a delay of approximately 130 μ s, there is an abrupt increase in signal. After peaking, the signals of both tracer and ablated

NaCl taper exponentially. The times for the signal to decay by half are 120 and 40 μ s for the NaCl and CH₃CN, respectively. The yields of laser-ablated NaCl and KCl measured with the laboratory FTMW cavity spectrometer are plotted in Figure 3.

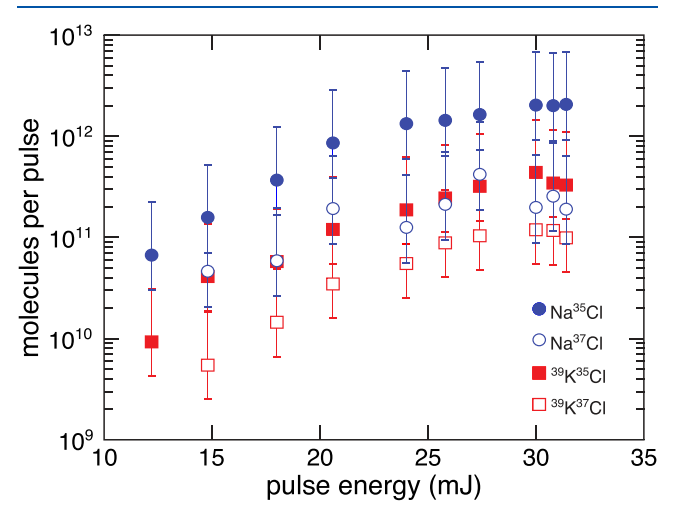


Figure 3. NaCl and KCl volatilization determined using the 13026.06, 12747.4 6, 15378.07, and 14940.91 MHz transitions for Na 35 Cl, Na 37 Cl, 39 K 35 Cl, and 39 K 37 Cl in the vibrational ground state, respectively. This measurement is made using a laboratory FTMW cavity spectrometer with an SO $_2$ calibrant. From the KCl FTmmW measurement, the temperature of the expansion is known to be approximately 6 K; error bars are yields determined at ± 3 K.

Using 100 to 500 averages, the threshold laser pulse energy for the detection of both salts is approximately 12 mJ. Between 12 and 30 mJ, the vapor yield for each of the isotopologues increases linearly. The ratios for Na³⁵Cl/Na³⁷Cl and $^{39}{
m K}^{35}{
m Cl}/^{39}{
m K}^{37}{
m Cl}$ are 0.86 \pm 0.13 and 0.78 \pm 0.10, respectively, compared with about 0.76 for the published natural abundance of chlorine.²³ These results depend on the rotational temperature of the expansion. Comparing the integrated intensities of the vibrational ground state rotational transitions of KCl measured using the FTmmW spectrometer with a simulation ²⁴ using catalog rotational constants B_0 , D_1 , and H_1 ²⁵ we know the ablation products are cooled to about 6 ± 3 K. The uncertainty of 3 K in rotational temperature is based on our prior experience with the carrier gas ablation source²⁶ and the differences between the sources used on the FTmmW and microwave experiments. As a check, a similar measurement was made using the FTmmW spectrometer by integrating the NaCl and CH₃CN traces in Figure 3. The result is also on the order of 10¹² NaCl molecules per pulse.

The positive ion mass spectra are shown in Figure 4. Although the rotational transitions of the main isotopologue of LiCl are about 6 GHz below the bottom edge of the FTmmW band, we include the LiCl ablation mass spectra as a matter of interest. With nanosecond pulses, we observe the metal ions for $^7\text{Li}^+$, Na $^+$, and both $^{39}\text{K}^+$ and $^{41}\text{K}^+$. The Faraday cup detector currents are 17, 0.9, 0.3, and 0.06 femtocoulombs per pulse, respectively. All three nanosecond spectra contain some additional peaks: at M/Z of 17 for LiCl and 48 for NaCl, as well as 24 and 48 for KCl. With femtosecond pulses, we observe the metal ions $^6\text{Li}^+$ and $^7\text{Li}^+$, Na $^+$, and $^{39}\text{K}^+$ and $^{41}\text{K}^+$. The Faraday cup detector currents for femtosecond ablation follow a reverse trend compared to the nanosecond ablation: 2.8, 8.4, and 11.0 for $^7\text{Li}^+$, Na $^+$, and $^{39}\text{K}^+$, respectively. The

femtosecond spectra have additional features of interest: peaks corresponding to triatomic ion clusters Li_2Cl^+ , Na_2Cl^+ , and K_2Cl^+ as well as their chlorine isotopologues. The ratios of the $^7\text{Li}^{12}$, $^3\text{Li}^{13}$, $^3\text{Li}^{14}$, $^$

Scanning electron microscopy images of nanosecond-ablated material collected on a witness plate are shown in Figure 5. Material from the NaCl and KCl targets have similar morphology to one another and look like liquid droplets that have resolidified after contact with the witness plate. ^{28,29} In particular, some of the larger particles (Figure 5a, center) exhibit thin wisps of splattered liquid salt emanating from the middle. A control experiment with a target made of paraffin wax showed no significant ejecta. Using a sample of about 100 imaged particles, the mean diameters of the splattered salts are about 500 nm (Figure 5c).

DISCUSSION

The center frequencies of the lines we observe agree with catalog values, ^{22,25} and we do not observe significant pressure or transit time broadening compared to what we have previously observed for stable gases, ^{4,5} which implies that the ablation products collide with the carrier gas and then expand together with it. Previous articles ^{4,5,18,30} discussed the small size and low power consumption of the FTmmW instrument and how it could be used to measure volatiles or stable atmospheric species *in situ*. ^{30,31} Our FTmmW detections of laser-volatilized NaCl and KCl demonstrate that the instrument can also be used to determine the molecular composition of condensed phases. Such a capability is complementary to mass spectrometry techniques, which are sensitive to ions, not neutral species. Prospective space deployments of the miniature FTmmW spectrometer could leverage existing flight-qualified laser³² and pump¹⁶ technologies.

The NaCl and KCl species we use in our experiments are themselves relevant to icy moons exploration as they are proxies for subsurface oceans in contact with rock.³³ In a future mission to the surface of an icy moon, a laser-ablation FTmmW spectrometer could potentially quantify salt isotopic abundance, which would constrain the salt origin. Other condensed-phase molecules might also be detectable provided they have rotational transition within the FTmmW bandwidth and are adequately polar.⁵

Salts and their byproducts have been observed at the moons of Saturn and Jupiter. Na_n(H₂O)⁺ and Na(NaOH)_n⁺ clusters as well as K+ have been identified at Enceladus using in situ mass spectrometry.³⁴ Salt-containing particles emanate from long-lived conduits in Enceladus' south pole that are probably shaped by tidal forcing.³⁵ Spectra of the plume material sampled by the Cassini spacecraft suggest multiple processes contribute to the ejection of salt-laden particles including clathrate decomposition and evaporation from a large, subsurface liquid-vapor interface. Particles associated with the latter process lead to a salinity estimate of the subsurface body of liquid: on the order of 1 mol NaCl per kilogram H₂O. While Cassini has been able to sample volatilized saltwater particles, much of the ejected materials are thought to be redeposited on the Enceledean crust, ³⁶ a hypothesis supported by the absence of appreciable atomic sodium vapor in Saturn's E-ring.³⁷ The redeposition of ejected salts motivates our interest in developing techniques for sampling solidsspecifically laser-ablation millimeter-wave spectrometry. Measurements of the types and concentrations of molecules on

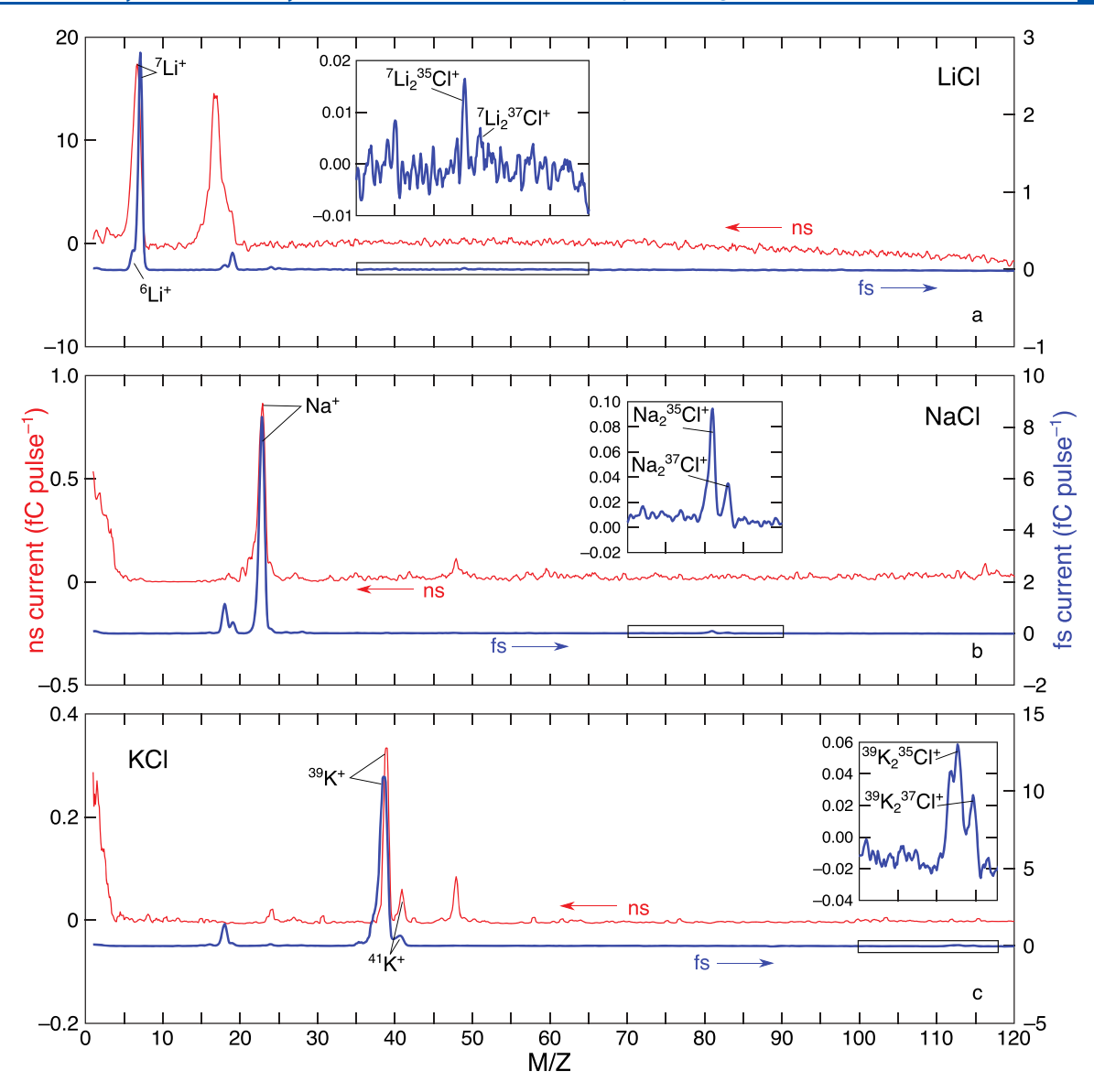


Figure 4. Positive ion mass spectra for nanosecond pulses (at 2 J cm^{-2} , 10 Hz) and femtosecond pulses (at 1 J cm^{-2} , 1 kHz) with (a) LiCl, (b) NaCl, and (c) KCl targets. Both pulse types yield positive metal ions. The femtosecond pulses also produce triatomic ions as shown in the highlighted insets. The vertical axis unit is femtocoulombs per pulse.

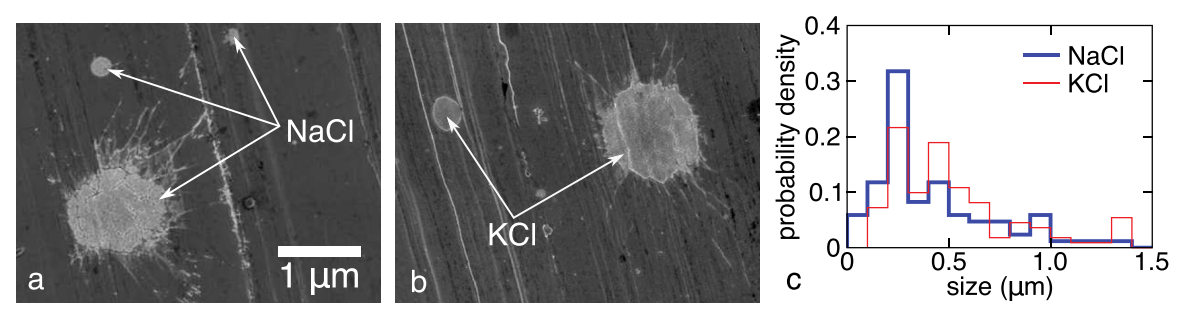


Figure 5. Scanning electron microscopy images of particles ablated from (a) NaCl and (b) KCl targets onto a coverslip after ablation by nanosecond pulses. The splatter implies the particles are liquid, which means that not all of the ejecta are converted to vapor. Future improvements to the ablation source should focus on more complete solid-to-vapor conversion since it is the vapor that contributes to the millimeter-wave signal. (c) Probability distribution of the diameter of the splattered particles. 100 J cm $^{-2}$ fluence, 3×10^{-6} Torr chamber pressure.

Enceladus' surface could yield new information about the ocean that is thought to have produced them. In particular, stratigraphy of those molecules, which is only possible through *in situ* probing, could inform us about how the ocean has

evolved over time. Surface deposits of salts, NaCl, KCl, and $MgCl_2$ also exist on Europa, where there is a question about whether the materials are evaporates³⁸ from a European ocean or radiolytically processed³⁹ deposits sputtered from Io's

volcanically derived atmosphere. Remote sensing of the condensed-phase materials suggests that the materials are indeed salts, but more specific characterization will likely require *in situ* analysis.

The small size of the FTmmW cavity allows us to use the delay of the mm-wave pulse to observe how the signal of the ablation products varies along the carrier gas beam. Because the NaCl is volatilized instantaneously, we know that the beam takes on the order 130 μ s to propagate from the source nozzle to the cavity. At the terminal speed of Ar gas expanding from a room temperature reservoir into vacuum, 41 the crossing time suggests the separation between the source nozzle and the cavity is about 70 mm, which agrees with the setup geometry although that distance was not precisely controlled during the experiment. The comparison with CH₃CN in Figure 2b indicates that the ablated salt is distributed along the beam. The argument for that conclusion goes as follows: The carrier gas pulse is approximately 500 µs long. The CH₃CN tracer occupies the entirety of the gas pulse because it is premixed, but the lifetime of its signal is just 40 μ s. The signal is probably truncated by the increase in temperature for the trailing portion of the gas pulse, which is an artifact of the finite vacuum pumping speed. The partition function of CH₃CN is sensitive to temperature: an increase in rotational temperature from 6 to 225 K reduces the signal by a factor of almost 300, which is on the order of the change we observe in Figure 2b. Compare this with a factor of 30 for NaCl over the same temperature range.²² We observe a sustained NaCl signal with an exponential decay (120 μ s) that is comparable to the CH₃CN one. The longer signal decay time for NaCl reflects the lower sensitivity to temperature, which implies that the salt vapor is dispersed in the carrier gas since the transit time through the cavity is on the order of just 20 μ s. That dispersion could happen because the volatilization from the pellet surface elapses over a finite time or because of diffusion in the beam. To evaluate which of these situations dominates, suppose that the salt vapor we observe volatilizes on the nanosecond time scale and consequently is injected into a small region of the carrier gas jet. The mean free path of ablated molecules enveloped in the carrier gas would be less than micrometer, so we do not expect dispersion due to the initial kinetic energy distribution. For a nominal binary diffusion coefficient of 1 × 10⁻⁴ m² s⁻¹, an instantaneous injection of salt molecules in the carrier gas beam would be dispersed over about 0.5 mm during the lifetime of the gas pulse, corresponding to about a 1- μ s passage at the carrier gas speed, so diffusion also probably does not explain the prolonged signal lifetime. Instead, we conclude that the salt vapor is probably volatilized over a sustained period of time from liquefied salt at the target surface or from particles like those we show in the Figure 5 micrographs. Ideally, the liquid would be converted to vapor to maximize the rotational signal. The droplet size distributions are similar for KCl and NaCl, which suggests the mechanics of their nanosecond ablation are similar.

The volatilization yields of NaCl and KCl we measure for nanosecond laser pulses are useful metrics. The yield measurements are validated by the fact that the chlorine isotope ratios are consistent with published natural abundance²³ within the experimental uncertainty. The linearity of the yield with pulse energy further validates the measurement since we expect the amount of vapor to increase with the strength of the pulse. The yield falloff above about 30 mJ, which is particularly apparent for the Na³⁷Cl, ³⁹K³⁵Cl, and

 39 K 37 Cl species, might be the result of marginal change in the exposed surface area of the liquefied material from which the salt vapor originates. Alternatively, the diminishing yield may be an artifact of an increasing rotational temperature at larger fluences, which could increase the average rotational temperature of the ablation products. Though still within the experimental uncertainty, the Na 35 Cl yield is consistently lower than the K 35 Cl yield across the pulse energies tested. Disparate physical properties could explain the difference. Another explanation is that the final temperature of the Na 35 Cl molecules after collisional cooling with the carrier gas is actually less than the 6 K temperature applied uniformly across the experiments. The temperature (T_p) of the ablated species after N collisions with a carrier gas at temperature T_c is 42

$$T_p(N) = T_c + [T_p(0) - T_c]e^{-N/\kappa}$$
 (1)

where κ is a mass parameter, $(m_c + m_p)^2/(2m_c m_p)$. For an expanded carrier gas temperature of 2 K and an initial temperature of the ablated species of 10^4 K, which are reasonable conditions for our experiment, $K^{35}Cl$ cools to 6 K after approximately 40 collisions. After the same number of collisions, $Na^{35}Cl$ in the beam would cool to approximately 3 K, which would lower the calibrated yields for that species by a factor of 3–8. If the lower $Na^{35}Cl$ temperature is confirmed with a future measurement, that correction would account for nearly all the difference we observe in Figure 2.

One reason for analyzing the ablation plume using mass spectrometry is to determine if ablation produces species that would complicate interpretation of the spectra. The positive metal ions in the Figure 4 mass spectra imply that some of the ablated material is chemically fragmented; however, these species lack a dipole moment and therefore would not radiate in the frequency range of our detector. The ion clusters observed in the femtosecond ablation plumes are too sparse to be detected rotationally. If we extrapolate the yields in Figure 3 to lower fluence, we find the ionization fraction for nanosecond pulses to be 10^{-7} to 10^{-6} . This ionization fraction estimate is probably a lower bound because not all ions couple into the Faraday cup detector. We do not observe salt ions (i.e., LiCl+, NaCl+, or KCl+) in the nanosecond nor the femtosecond mass spectra. A possible explanation for the absence of salt ions is that their ground state potential energy curves do not contain a stable atomic spacing and therefore dissociate upon ionization.⁴³ It is also possible that the ions form by dissociation from a neutral excited state or by collisional dissociation within the ablation plume.

The triatomic ion clusters Na_2Cl^+ and K_2Cl^+ that are seen with femtosecond pulses are interesting because they suggest that chemistry can occur during the ablation process. These particular clusters have been observed previously by Chupka⁴⁴ in mass spectra of molecular beams produced using an oven source. Future development of the laser-ablation source for *in situ* FTmmW spectroscopy should address the likelihood that chemistry occurs in the ablation plume, particularly for larger organic molecules. In the case of salts, the triatomic clusters are in trace abundance.

Comparing the capability of a laser-ablation outfitted FTmmW spectrometer to other techniques, we assert that its greatest strength is the specificity with which it can identify a particular molecule. Even with the modest 200- to 300-kHz line widths we observe with our FTmmW setup, the precision of our measurements is better than one part in 10^4 and can

easily distinguish molecules and isotopologues. NASA is currently developing laser-ablation mass spectrometry for flight deployment. 45 In general, mass spectrometry is complementary to rotational spectroscopy. While mass spectrometry is sensitive to a small number of ions, it is typically not as good as rotational spectroscopy at distinguishing different species. In general, in situ analysis of salts at icy moons is preferable to existing remote measurements. To date, fitting the spectral features of remote infrared reflectance spectra for salts on the surfaces of icy moons has been inconclusive. 38,46 The laser ablation mass spectrometry and rotational spectroscopy techniques would provide a localized. definitive measurement of salt composition if performed on an icy moon. In principal, the laser-ablation source lends itself to standoff detection, which simplifies the sample handling requirements; however, some future design work would be needed to align the collisional cooling jet with the ablation plume and FT cavity in a fielded instrument.

In addition to the salts, there are a number of sites throughout the solar system where a laser-ablation-coupled FTmmW spectrometer could be used to analyze condensed-phase organic molecules, such as Saturn's moon Titan and comets. 47,48 In future work with the FTmmW spectrometer, we hope to detect polyatomic laser-ablated molecules including organics.

CONCLUSION

We coupled a new Fourier transform millimeter-wave spectrometer intended for doing *in situ* spectroscopy in space to a collisional-cooling laser-ablation source. Along with its small size, a strength of the device is the specificity with which it identifies the composition of volatilized species inside its cavity. We show that the new device can be used to determine the molecular composition of solids. We have demonstrated that capability using NaCl and KCl targets, which are interesting for their relevance to icy moons and the putative subsurface oceans. Nanosecond ablation of the salts produces metal ions and liquefied particles, which we hope to mitigate with future refinements to the wavelength and pulse duration of the ablation source. We plan to pursue detections of laser-ablated organic molecules as part of future work.

AUTHOR INFORMATION

Corresponding Author

Brian J. Drouin — Jet Propulsion Laboratory, California Institute of Technology, Pasadena, California 91109-8909, United States; orcid.org/0000-0002-9125-2822; Email: Brian.J.Drouin@jpl.nasa.gov

Authors

Alexander W. Raymond — Center for Astrophysics | Harvard & Smithsonian, Cambridge, Massachusetts 02138, United States Kin Long Kelvin Lee — Center for Astrophysics | Harvard & Smithsonian, Cambridge, Massachusetts 02138, United States Michael C. McCarthy — Center for Astrophysics | Harvard & Smithsonian, Cambridge, Massachusetts 02138, United States; John A. Paulson School of Engineering and Applied Sciences, Harvard University, Cambridge, Massachusetts 02138, United States; Occid.org/0000-0001-9142-0008

Eric Mazur — John A. Paulson School of Engineering and Applied Sciences and Department of Physics, Harvard University, Cambridge, Massachusetts 02138, United States; orcid.org/0000-0003-3194-9836

Complete contact information is available at: https://pubs.acs.org/10.1021/acs.jpca.9b10548

Notes

The authors declare no competing financial interest.

ACKNOWLEDGMENTS

A.W.R. gratefully acknowledges the support of the NASA Space Technology Research Fellowship, Grant No. NNX13AM67H. SEM imaging was done at the Center for Nanoscale Systems (CNS), a member of the National Nanotechnology Infrastructure Network (NNIN), which is supported by the National Science Foundation under NSF Award no. 1541959. Portions of the research described in this paper were performed at the Jet Propulsion Laboratory, California Institute of Technology, with support from the National Aeronautics and Space Administration under Grant No. NNN13D485T issued by the Planetary Science Division PICASSO program. M.C.M. and K.L.K.L. acknowledge NSF Grants AST-1615847 and CHE-1566266, and NASA grants NNX13AE59G and 80NSSC18K0396 for financial support. We thank Deacon Nemchick and Timothy Crawford their help with the FTmmW setup and Weilu Shen for her feedback on the manuscript.

REFERENCES

- (1) Castillo, J. C.; Bar-Cohen, Y.; Vance, S.; Choukroun, M.; Lee, H. J.; Trainer, M. G.; Getty, S. A. In *Low temperature materials and mechanisms*; Bar-Cohen, Y., Ed.; CRC Press: Boca Raton, 2016; Chapter 9, pp 1–42.
- (2) Zolotov, M. Y. An oceanic composition on early and today's Enceladus. *Geophys. Res. Lett.* **2007**, *34*, GL031234.
- (3) Drouin, B. J.; Tang, A.; Schlecht, E.; Brageot, E.; Gu, Q. J.; Ye, Y.; Shu, R.; Frank Chang, M.-C.; Kim, Y. A CMOS millimeter-wave transceiver embedded in a semi-confocal Fabry-Perot cavity for molecular spectroscopy. *J. Chem. Phys.* **2016**, *145*, 074201.
- (4) Raymond, A. W.; Drouin, B. J.; Tang, A.; Schlecht, E.; Mazur, E. Miniature cavity for in situ millimeter wave gas sensing: N₂O and CH₃OH detection. *Sens. Actuators, B* **2018**, 254, 763–770.
- (5) Nemchick, D. J.; Drouin, B. J.; Cich, M. J.; Crawford, T.; Tang, A. J.; Kim, Y.; Reck, T. J.; Schlecht, E. T.; Chang, M.-C. F.; Virbila, G. A 90–102 GHz CMOS based pulsed Fourier transform spectrometer: New approaches for *in situ* chemical detection and millimeter-wave cavity-based molecular spectroscopy. *Rev. Sci. Instrum.* **2018**, *89*, 073109.
- (6) Townes, C. H.; Schawlow, A. L. Microwave spectroscopy; Dover Publications: New York, 1975.
- (7) Blanco, S.; Lesarri, A.; López, J. C.; Alonso, J. L. The gas-phase structure of alanine. *J. Am. Chem. Soc.* **2004**, *126*, 11675–11683.
- (8) Perez, C.; Mata, S.; Blanco, S.; Lopez, J. C.; Alonso, L. Jet-cooled rotational spectrum of laser-ablated phenylalanine. *J. Phys. Chem. A* **2011**, *115*, 9653–9657.
- (9) Grubbs, G.; Frohman, D. J.; Novick, S. E.; Cooke, S. Measurement and analysis of the pure rotational spectra of tin monochloride, SnCl, using laser ablation equipped chirped pulse and cavity Fourier transform microwave spectroscopy. *J. Mol. Spectrosc.* **2012**, 280, 85–90.
- (10) Zaleski, D. P.; Tew, D. P.; Walker, N. R.; Legon, A. C. Chemistry in laser-Induced plasmas: formation of M−C≡C−Cl (M = Ag or Cu) and their characterization by rotational spectroscopy. *J. Phys. Chem. A* **2015**, *119*, 2919–2925.
- (11) Walker, N. R.; Tew, D. P.; Harris, S. J.; Wheatley, D. E.; Legon, A. C. Characterisation of H_2S ···CuCl and H_2S ···AgCl isolated in the gas phase: A rigidly pyramidal geometry at sulphur revealed by rotational spectroscopy and *ab initio* calculations. *J. Chem. Phys.* **2011**, 135, 014307.

- (12) Brünken, S.; Müller, H. S. P.; Menten, K. M.; McCarthy, M. C.; Thaddeus, P. The rotational spectrum of TiO₂. *Astrophys. J.* **2008**, 676, 1367–1371.
- (13) Halfen, D. T.; Ziurys, L. M. The pure rotational spectrum of the T-shaped AlC₂ radical (\tilde{X}^2 A₁). Phys. Chem. Chem. Phys. **2018**, 20, 11047–11052.
- (14) Klein, H. P. The Viking biological experiments on Mars. *Icarus* 1978, 34, 666–674.
- (15) Lebreton, J.-P.; Witasse, O.; Sollazzo, C.; Blancquaert, T.; Couzin, P.; Schipper, A.-M.; Jones, J. B.; Matson, D. L.; Gurvits, L. I.; Atkinson, D. H.; et al. An overview of the descent and landing of the Huygens probe on Titan. *Nature* **2005**, *438*, 758–764.
- (16) Mahaffy, P. R.; Webster, C. R.; Cabane, M.; Conrad, P. G.; Coll, P.; Atreya, S. K.; Arvey, R.; Barciniak, M.; Benna, M.; Bleacher, L.; et al. The Sample Analysis at Mars investigation and instrument suite. *Space Sci. Rev.* **2012**, *170*, 401–478.
- (17) Meslin, P.-Y.; Gasnault, O.; Forni, O.; Schroder, S.; Cousin, A.; Berger, G.; Clegg, S. M.; Lasue, J.; Maurice, S.; Sautter, V.; et al. Soil diversity and hydration as observed by ChemCam at Gale Crater, Mars. *Science* **2013**, *341*, 1238670–1238670.
- (18) Raymond, A. W.; Drouin, B. J.; Tang, A.; Schlecht, E.; Kim, Y.; Chang, M.-C. F. *In situ* gas sensing with a 100 GHz CMOS spectrometer. 2017 *IEEE Aerospace Conference* 2017, 1–7.
- (19) Grabow, J.-U.; Palmer, E. S.; McCarthy, M. C.; Thaddeus, P. Supersonic-jet cryogenic-resonator coaxially oriented beam-resonator arrangement Fourier transform microwave spectrometer. *Rev. Sci. Instrum.* 2005, 76, 093106.
- (20) Caris, M.; Lewen, F.; Winnewisser, G. Pure rotational spectroscopy of sodium chloride, NaCl, up to 930 GHz. Z. Naturforsch., A: Phys. Sci. 2002, 57, 2001.
- (21) Caris, M.; Lewen, F.; Müller, H.; Winnewisser, G. Pure rotational spectroscopy of potassium chloride, KCl, up to 930 GHz and isotopically invariant analysis of KCl and NaCl. *J. Mol. Struct.* **2004**, *695*–*696*, 243–251.
- (22) Müller, H. S.; Schlöder, F.; Stutzki, J.; Winnewisser, G. The Cologne Database for Molecular Spectroscopy, CDMS: a useful tool for astronomers and spectroscopists. *J. Mol. Struct.* **2005**, *742*, 215–227
- (23) Meyerson, S. Natural abundance of chlorine isotopes. *Anal. Chem.* **1961**, 33, 964–964.
- (24) Western, C. M. PGOPHER: A program for simulating rotational, vibrational and electronic spectra. *J. Quant. Spectrosc. Radiat. Transfer* **2017**, 186, 221–242.
- (25) Pickett, H.; Poynter, R.; Cohen, E.; Delitsky, M.; Pearson, J.; Müller, H. Submillimeter, millimeter, and microwave spectral line catalog. *J. Quant. Spectrosc. Radiat. Transfer* **1998**, *60*, 883–890.
- (26) Zingsheim, O.; Martin-Drumel, M.-A.; Thorwirth, S.; Schlemmer, S.; Gottlieb, C. A.; Gauss, J.; McCarthy, M. C. Germanium dicarbide: evidence for a T-Shaped ground state structure. J. Phys. Chem. Lett. 2017, 8, 3776–3781.
- (27) Pearson, E. F.; Gordy, W. Millimeter- and submillimeter-wave spectra and molecular constants of LiF and LiCl. *Phys. Rev.* **1969**, *177*, 52–58
- (28) Raymond, A. W.; Mazur, E. Imaging nanosecond ablation of copper at low ambient pressure. *Conference on Lasers and Electro-Optics* **2017**, STh1J.S.
- (29) Raymond, A. W. Laser ablation millimeter-wave instrumentation for in situ exploration of the solar system. Ph.D. Thesis; Harvard University: 2018.
- (30) Drouin, B. J.; Cooper, K.; Dengler, R.; Chavez, M.; Chun, W.; Crawford, T. Submillimeter wave spectrometry for *in-situ* planetary science. 2012 IEEE Aerospace Conference 2012, 1–4.
- (31) Drouin, B. J.; Cooper, K.; Stachnik, R. A.; Pearson, J. C. Submillimeter wave spectroscopy and the search for life on planets. 2008 33rd International Conference on Infrared, Millimeter and Terahertz Waves 2008, 1–3.
- (32) Maurice, S.; Wiens, R. C.; Saccoccio, M.; Barraclough, B.; Gasnault, O.; Forni, O.; Mangold, N.; Baratoux, D.; Bender, S.; Berger, G.; et al. The ChemCam instrument suite on the Mars

- Science Laboratory (MSL) Rover: Science objectives and mast unit description. Space Sci. Rev. 2012, 170, 95–166.
- (33) Postberg, F.; Schmidt, J.; Hillier, J.; Kempf, S.; Srama, R. A saltwater reservoir as the source of a compositionally stratified plume on Enceladus. *Nature* **2011**, *474*, 620–622.
- (34) Postberg, F.; Kempf, S.; Schmidt, J.; Brilliantov, N.; Beinsen, A.; Abel, B.; Buck, U.; Srama, R. Sodium salts in E-ring ice grains from an ocean below the surface of Enceladus. *Nature* **2009**, *459*, 1098–1101.
- (35) Kite, E. S.; Rubin, A. M. Sustained eruptions on Enceladus explained by turbulent dissipation in tiger stripes. *Proc. Natl. Acad. Sci. U. S. A.* **2016**, *113*, 3972–3975.
- (36) Schmidt, J.; Brilliantov, N.; Spahn, F.; Kempf, S. Slow dust in Enceladus' plume from condensation and wall collisions in tiger stripe fractures. *Nature* **2008**, *451*, 685–688.
- (37) Schneider, N. M.; Burger, M. H.; Schaller, E. L.; Brown, M. E.; Johnson, R. E.; Kargel, J. S.; Dougherty, M. K.; Achilleos, N. A. No sodium in the vapour plumes of Enceladus. *Nature* **2009**, 459, 1102–
- (38) Brown, M. E.; Hand, K. P. Salts and radiation production products on the surface of Europa. Astron. J. 2013, 145, 110.
- (39) Thomas, E. C.; Hodyss, R.; Vu, T. H.; Johnson, P. V.; Choukroun, M. Composition and evolution of frozen chloride brines under the surface conditions of Europa. *ACS Earth and Space Chemistry* **2017**, *1*, 14–23.
- (40) Lellouch, E.; Paubert, G.; Moses, J. I.; Schneider, N. M.; Strobel, D. F. Volcanically emitted sodium chloride as a source for Io's neutral clouds and plasma torus. *Nature* **2003**, *421*, 45–47.
- (41) Morse, M. D. Supersonic Beam Sources. *Exp. Methods Phys. Sci.* **1996**, 29, 21–47.
- (42) Hutzler, N. R.; Lu, H. I.; Doyle, J. M. The buffer gas beam: An intense, cold, and slow source for atoms and molecules. *Chem. Rev.* **2012**, *112*, 4803–4827.
- (43) Dietrich, P.; Corkum, P. B. Ionization and dissociation of diatomic molecules in intense infrared laser fields. *J. Chem. Phys.* **1992**, 97, 3187–3198.
- (44) Chupka, W. A. Dissociation energies of some gaseous alkali halide complex ions and the hydrated ion $K(H_2O)^+$. J. Chem. Phys. 1959, 30, 458–465.
- (45) Getty, S. A.; Elsila, J.; Balvin, M.; Brinckerhoff, W. B.; Cornish, T.; Li, X.; Ferrance, J.; Grubisic, A.; Southard, A. Molecular Analyzer for Complex Refractory Organic-Rich Surfaces (MACROS). 2017 IEEE Aerospace Conference 2017, 1–11.
- (46) Spencer, J. R.; Nimmo, F. Enceladus: an active ice world in the Saturn system. *Annu. Rev. Earth Planet. Sci.* **2013**, *41*, 693–717.
- (47) Raymond, A. W.; Sciamma-O'Brien, E.; Salama, F.; Mazur, E. A model of Titan-like chemistry to connect experiments and Cassini observations. *Astrophysical Journal* **2018**, *853*, 107.
- (48) Capaccioni, F.; Coradini, A.; Filacchione, G.; Erard, S.; Arnold, G.; Drossart, P.; De Sanctis, M. C.; Bockelee-Morvan, D.; Capria, M. T.; Tosi, F. The organic-rich surface of comet 67P/Churyumov-Gerasimenko as seen by VIRTIS/Rosetta. *Science* 2015, 347, aaa0628.